FORECASTING BREAKING WAVES DURING STORMS

Michael Banner, Ekaterini Kriezi and Russel Morison

Centre for Environmental Modelling and Prediction
School of Mathematics, The University of New South Wales
Sydney, Australia

1. INTRODUCTION

The occurrence and consequences of large breaking waves has been a persistent concern for centuries of seafarers and coastal dwellers. These waves are responsible for the greatest dynamic loading on ships and coastal structures, and can present a significant risk to human safety on smaller vessels. Also, air-sea interaction scientists have long sought to understand which environmental processes and variables control the relative occurrence rate (probability) and strength of breaking of the dominant sea waves. This applies not only to the dominant waves, but also to the shorter breaking waves in the spectrum. Motivation for the inclusion of shorter breaking waves includes improved modeling for the following key processes at the air-sea interface: the aerodynamic consequences (air-flow separation) for the wind input source function and sea surface drag coefficient; enhanced upper ocean mixing; increased air-sea fluxes of low-solubility gases and spray.
Our recent results from a number of diverse studies provide encouraging guidance on which processes need to be included to be able to quantify wave breaking from forecast models. This paper aims to highlight recent progress on our ongoing efforts towards this goal.

Applications of this work include routine sea state forecasts of dangerous breaking wave conditions, as well as improved coupled modelling of air-sea fluxes and upper ocean mixing processes, including foam cover.

2. BACKGROUND

In Fig. 6 of his recent review paper, Donelan (1998) shows that more than 97% of the energy input from the wind to the sea surface ends up as turbulence in the water, mediated predominantly through wave breaking. At which wave scales does this occur? While the details remain to be refined, recent data shows that the breaking occurs on a wide range of spatial wave scales, as seen in the typical frequency distributions reported by Ding and Farmer (1994) for open ocean conditions and wind speeds from 6 to 12 m/s. The detected breaking events had a broad distribution of length scales, with the majority of breaking waves having speeds in the range 3-5 m/s, corresponding to waves much shorter than the dominant waves. This was confirmed in more recent measurements (Gemmrich, private communication). Thus wave breaking and dissipation occur over a wide range of spectral scales, resulting primarily from the rate at which the whitecap does work against the orbital motion of the underlying breaking wave. There will also be a background decay of wave energy in the turbulent ocean surface layer left behind by the breakers.

Observations from dedicated studies of ocean wave breaking indicate that neither wind speed nor spectral peak inverse wave age, U/c_p, correlate successfully with breaking probability (Gemmrich and Farmer, 1999). Also, Holthuijsen and Herbers (1986) observed that local wave properties such as individual wave steepness are not able to separate breaking and non-breaking waves from observed wave height versus wave period distributions. In any event, such local indicators provide no dynamical basis for diagnosing breaking onset.

2.1 Wave groups and wave breaking

A significant association of wave breaking with ocean wave groupiness was first noted in the literature in Donelan et al. (1972) and investigated in detail by Holthuijsen and Herbers (1986), who found a remarkably strong correlation between wave breaking and wave group structure. These findings suggest we should take a more global view of breaking rather than just considering local criteria, and look more closely at *group behaviour*.

2.2 Insight from modelling 2D nonlinear groups

Song and Banner (2002) and Banner and Song (2002) used two-dimensional 'exact' Euler equation boundary element codes (periodic domain and numerical wave tank) to track the evolution of wave group maximum and the associated local depth-integrated energy density, E. It was observed that, travelling with the group, there is a significant flux of energy towards the centre of the group - not a *steady* flux, but an oscillatory flux, due to the crest-trough asymmetry of the waveform. Thus

from this viewpoint, there are intrinsically two timescales involved in the process.

It was proposed that the onset of breaking is linked to a threshold in the slower flux, i.e. the mean convergence rate of wave-coherent normalized energy Ek^2 at the envelope maximum. Here k is the local carrier wavenumber and $<E>$ is the mean energy of the wave group. From our results, for the typical wave groups studied, there appears to be a *threshold* non-dimensional growth rate for the local non-dimensional energy density, that can distinguish wave groups that evolve to break from those that relax without breaking, i.e. undergo 'recurrence'.

2.3 Recent observations

It is well known that dominant sea waves routinely occur in wave groups, so are the ideas arising from 2-D modelling helpful? In particular, is there a parametric threshold for breaking and if so, how can we parameterise most simply the underlying nonlinearity of the waves?

The mean wave steepness is the traditional parameter used in classical wave train perturbation analysis, so this should provide an initial parameter to investigate. Following up on this possibility for the dominant sea waves, Banner et al. (2000) found a strong correlation and clear threshold behaviour as a result of relating breaking probability to the significant mean steepness (defined below) of the dominant waves. Averages over records sufficiently longer than the usual 20 minute wave records were needed to include enough wave *groups* to gather stable statistics. The breaking probability was defined as the ratio of the passage rate of breaking crests to total crests past a fixed point, in spectral peak enhancement region.

2.4 Wave breaking probability in the spectrum

This may be defined as the ratio of the passage rate past a fixed point of breaking crests with velocities in (**c**, **c+dc**) to the passage rate past a fixed point of all wave crests with velocities in (**c, c+dc**).

The breaking probability for wave scale c is then quantified as:

$$f_{\mathrm{RWR}}(\mathbf{c}) = \frac{\int \mathrm{c}\Lambda(\mathbf{c})\,\mathrm{d}\mathbf{c}}{\int \mathrm{c}\Pi(\mathbf{c})\,\mathrm{d}\mathbf{c}}$$

where $\Lambda(\mathbf{c})$ = spectral density of *breaking wave* crest length per unit area with velocities in the range (**c, c+dc**) and $\Pi(\mathbf{c})$ = spectral density of the *total wave* crest length per unit area with velocities in the range (**c, c+dc**). Also f_{RWR} is the breaking probability in which the denominator is quantified using the Riding Wave Removal crest counting technique (Banner et al., 2002).

To quantify the mean nonlinearity of the waves, including the higher wavenumber components above the spectral peak, following Banner et al., (2002), we used the azimuth-integrated spectral saturation $\sigma(k) = k^4 \int F(\boldsymbol{k})\,\mathrm{d}\boldsymbol{k} = (2\pi)^4 f^5 F(f) / 2g^2$. This is an alternative to the significant steepness $H_s * k_p/2$, which is only applicable at the spectral peak. Here $F(\boldsymbol{k})$ and $F(f)$ are the wave enrgy spectra as a function of wavenumber and frequency, respectively, H_s is the significant wave height and k_p is the spectral peak wavenumber.

The use of the azimuth-integrated saturation $\sigma(k)$ is complicated by broader 'directional spreading' as the wavenumber increases above the spectral peak. However, the same qualitative threshold behaviour is evident (Banner et al., 2002) once the spectral saturation $\sigma(k)$ is normalized by the mean directional spreading width at the spectral peak $\overline{\theta}_P$ to provide the normalised spectral saturation $\tilde{\sigma}(k)$. Observed breaking probabilities for different centre frequencies relative to the spectral peak were constructed and found to have a well-defined threshold behaviour, with a common breaking threshold value $\tilde{\sigma}_T \sim 0.005$, as seen in Figure 1.

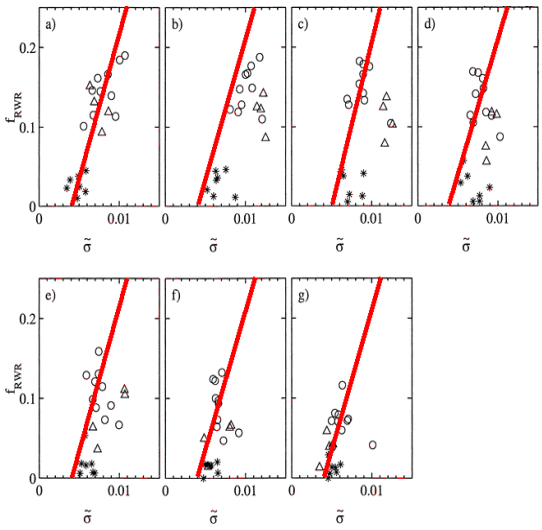

Figure 1. Breaking probability f_{RWR} against $\tilde{\sigma}$, the azimuth-integrated saturation normalized by the mean spectral spreading width $\overline{\theta}_P$ at the spectral peak for the range of non-dimensional centre frequencies f_c/f_p investigated: (a) f_c/f_p = 1.0 (b) f_c/f_p = 1.16 (c) f_c/f_p = 1.35 (d) f_c/f_p = 1.57 (e) f_c/f_p = 1.83 (f) f_c/f_p = 2.13 (g) f_c/f_p = 2.48. Each data point is from a one-hour data record from three N. Pacific storms, as described in Banner et al. (2002). Note the strong threshold behavior and

close correspondence in the specified spectral bands.

3. WAVE MODEL IMPLEMENTATION

3.1 Radiative transfer equation

The radiative transfer equation (deep water, no currents) for describing the evolution of the waveheight spectrum $F(k)$ is given by

$$\frac{\partial F}{\partial t} + \boldsymbol{c}_g \cdot \nabla F = S_{tot}$$

where $F = F(k,\theta)$ is the directional wave spectrum, $\boldsymbol{c}_g$ is the group velocity, $S_{tot} = S_{in} + S_{nl} + S_{ds}$ is the total source term, in which S_{in} is the atmospheric input spectral source term, S_{nl} is the nonlinear spectral transfer source term representing nonlinear wave-wave interactions within the spectrum, and S_{ds} is the spectral dissipation rate primarily due to wave breaking.

3.2 New spectral dissipation rate term S_{ds}

From our new insight into the physics of breaking onset, we have developed a refined form of $S_{ds}(\boldsymbol{k})$ embodying the strong saturation threshold behaviour described above in section 2.4. It is based on treating waves in different directional spectral bands as nonlinear wave groups. In the form of S_{ds}, shown below, we used a power law function of the spectral saturation ratio to reflect the observed threshold behaviour, refining the form proposed in Alves and Banner (2003):

$$S_{ds}(\boldsymbol{k}) = C[(\tilde{\sigma} - \tilde{\sigma}_T)/\tilde{\sigma}_T)^a + E_{res}]\sigma^b(\tilde{\sigma}/\tilde{\sigma}(\boldsymbol{k_m})^c \omega F(\boldsymbol{k})$$

where E_{res} is a background residual dissipation coefficient parameterised by the dominant wave steepness, and $\boldsymbol{k}_m$ is the mean wavenumber given by $\int \boldsymbol{k} F(\boldsymbol{k})\, d\boldsymbol{k} / \int F(\boldsymbol{k})\, d\boldsymbol{k}$. The exponents a, b, c and coefficient C were chosen by matching to the observed fetch evolution of the total energy and to the expected high wavenumber form of $S_{in}(\boldsymbol{k})$.

3.3 Wide bandwidth computation of fetch-limited wind wave evolution

A new proposed form for S_{ds} is based on the local saturation ratio, as described above. This in contrast to the integral wave steepness used in the quasi-linear form of S_{ds} presently used in most operational wave models. As evidenced by the excellent reproduction (see Figure 2 below) of the observed growth curves compiled by Kahma and Calkoen (1992), this new form has much greater flexibility to model S_{ds} within the spectrum over the full range of sea states from young to old.

To illustrate the methodology, computations of the directional wave spectrum were made for the spectral bandwidth covering 0.03 Hz to 3 Hz, for a forcing wind speed of U_{10} = 10 m/s. For this calculation, we used a standard parametric form of S_{in} due to Yan (1987), a form of the 'exact' nonlinear transfer source term S_{nl} due to Resio (private communication) and the form of S_{ds} described in 3.2 above.

Typical correspondence between computed and observed integral wave properties for fetch-limited evolution is seen in the non-dimensional evolution curves in Figure 2 below. The model reproduces closely the observed evolution of mean wave energy and dominant frequency, as collated by Kahma and Calkoen (1992).

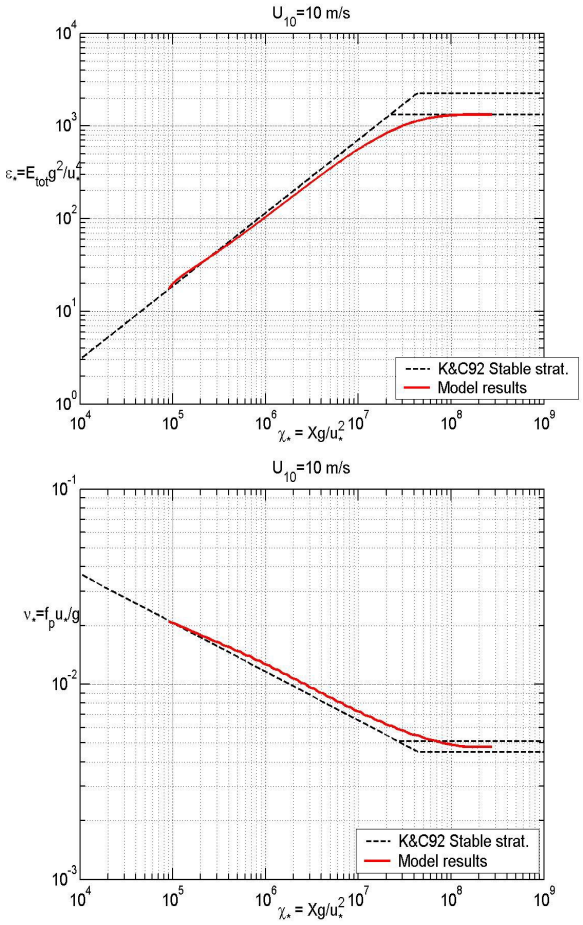

Figure 2. The close correspondence between model results using our saturation-threshold dissipation rate term and the observed fetch-limited evolution of non-dimensional wave energy ε_* (upper panel) and nondimensional peak frequency ν_* (lower panel) against nondimensional fetch χ_*, based on friction velocity u_* scaling. The dashed growth curve is the Kahma-Calkoen (1992) empirical data correlation. The horizontal dashed asymptotes represent the Pierson-Moskowitz (PM)

full development limits for non-dimensional wave energy (left panel) and peak frequency (right panel). The lower horizontal asymptotes in the each panel are the modified PM limit proposed by Alves et al. (2003).

3.4 Forecasting the breaking probability of dominant waves

To extract breaking probabilities for the dominant wind waves, the relationship based on the data in Figure 1 is used as a look-up table. This empirical relationship, proposed as a common breaking probability threshold in terms of the normalized saturation $\tilde{\sigma}(k)$ for all wave scales in the computational domain, is shown graphically in Figure 3.

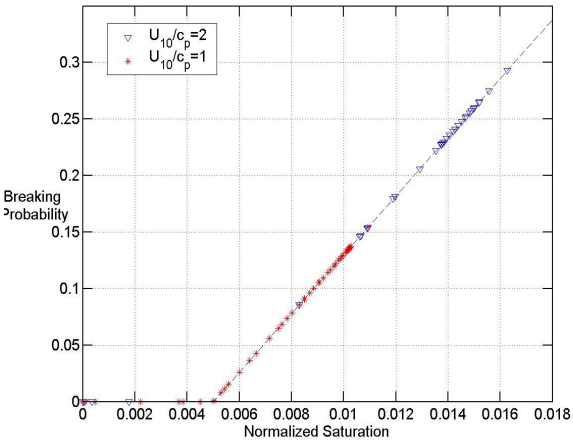

Figure 3. Assumed model threshold function for breaking probability at any wave scale against the local normalised spectral saturation at that scale. The symbols show the computed breaking probabilities for a young and an old wind sea during a run with U_{10}=10 m/s.

The directional frequency spectrum computed by the model at any stage of development is used to calculate its fifth moment (the saturation) and also its directional spreading width. The breaking probability of the dominant seas then follows from the normalized saturation at the spectral peak, via the look-up table. Figure 4 shows the variation of the normalized spectral saturation $\tilde{\sigma}$ as the wind sea develops. Note in particular how the dominant wave (k/k_p=1) saturation decreases with wave age from 0.016 to below 0.004. Accordingly, the dominant wave breaking probability is predicted to decrease from about 25% to zero. For reference, Figure 4 illustrates computed loci of breaking probabilities for young and old wind sea runs.

3.5 Present status

Further calculations at other wind speeds and wave ages are proceeding, particularly for higher wind speeds to address severe sea state conditions. A thorough field validation is essential before this product can be added to routine sea state forecasts. A companion breaking measurement program is currently being implemented on a Bass Strait gas platform to validate this proposed methodology over a year of storms.

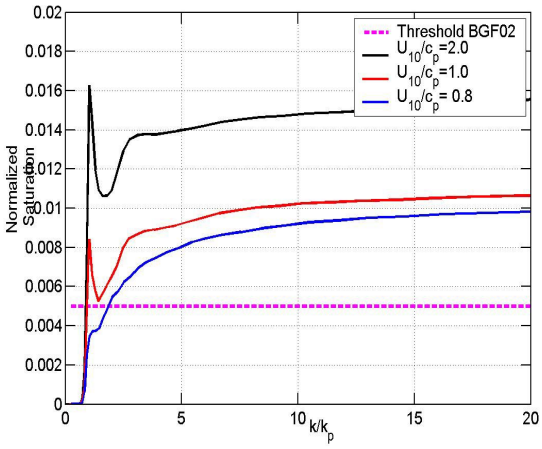

Figure 4. Variation with distance (k/k_p) from the spectral peak wavenumber of the normalised spectral saturation $\tilde{\sigma}$ as the wind sea develops. Note in particular how the dominant wave (k/k_p=1) saturation decreases with wave age from 0.016 to below 0.004. The predicted dominant wave breaking probability follows from Figure 3.

4. CONCLUDING REMARKS

Our approach identifies nonlinear wave group dynamics as the *primary* mechanism involved in the breaking onset of 2-D deep water waves. In this framework, there appears to be a common threshold for a dimensionless mean growth rate, reflecting the mean convergence rate of energy at the envelope maximum, which separates breaking from recurrent evolution. It is applicable in the presence of strong forcing by wave-slope-coherent surface pressure and surface layer shear.

For the dominant wind sea, a threshold significant wave steepness relationship appears to be a good first approximation for correlating breaking probability. For different wave scales, observations indicate that if the normalised spectral saturation is used to quantify the nonlinearity, breaking probability curves show self-similar threshold behaviour at different scales. A refined form for S_{ds} based on these observations appears to perform well in reproducing observed behaviour both at the

spectral peak (integral fetch growth curves) and also at the spectral tail (level, directional spreading).

Here, we are seeking to be able to provide, for the first time, reliable predictions of the spectral properties of shorter breaking waves. Comparison of our initial computational results of these breaking wave properties with recent field data is encouraging, and has the potential to improve the reliability of air-sea interaction models, especially for severe sea state conditions.

Acknowledgements

The financial support for this project provided by the Australian Research Council and the US Office of Naval Research is gratefully acknowledged.

References

Alves, J.H and M.L. Banner, 2003. Performance of a saturation-based dissipation source term for wind wave spectral modelling. J. Phys. Oceanogr. 33, 1274-1298

Alves, J.H., M.L. Banner and I.R. Young, 2003: Revisiting the asymptotic limits of fully-developed wind seas. J. Phys. Oceanogr., 33, 1301-1323.

Banner, M.L., J.R. Gemmrich and D.M. Farmer, 2002: Multiscale measurements of ocean wave breaking probability. J. Phys. Oceanogr. 32, 3364-3375

Banner, M.L. & J. Song, 2002: On determining the onset and strength of breaking for deep water waves. Part 2: Influence of wind forcing and surface shear. J. Phys. Oceanogr., 32, 2559-2570

Banner, M.L., A.V. Babanin and I.R. Young, 2000: Breaking probability for dominant waves on the sea surface. J. Phys. Oceanogr., 30, 3145-3160.

Ding, L. and D.M. Farmer, 1994: Observations of breaking surface wave statistics. J. Phys. Oceanogr., 24, 1368-1387.

Donelan, M.A., M.S. Longuet-Higgins, and J.S. Turner, 1972: Whitecaps. Nature 239, 449-451

Donelan, M.A., 1998: Air-water exchange processes. In *Physical Processes in Oceans and Lakes* (Ed.: J. Imberger), AGU Coastal and Estuarine Studies 54, 19-36.

Gemmrich, J.R and D.M. Farmer, 1999: Observations of the scale and occurrence of breaking surface waves. J. Phys. Oceanogr. 29, 2595-2606

Holthuijsen, L.H., and T.H.C. Herbers, 1986: Statistics of breaking waves observed as whitecaps in the open sea. J. Phys. Oceanogr., 16, 290-297

Hwang, P.A., D.W. Wang, E.J. Walsh, W.B. Krabill & R.W. Swift, 2000: Airborne measurements of the wavenumber spectra of ocean surface waves. Part II: Directional distribution. J. Phys. Oceanogr., 30, 2768-2787

Kahma, K. and C.J. Kalkoen, 1992: Reconciling differences in the observed growth of wind-generated waves. J. Phys. Oceanogr., 22, 1389-1405

Melville, W.K. and P. Matusov, 2002: Distribution of breaking waves at the ocean surface. Nature, 417, 58-63

Song, J-B and M. L. Banner, 2002: On determining the onset and strength of breaking for deep water waves. Part 1: Unforced irrotational wave groups. J. Phys. Oceanogr, 32, 2541-2558

Yan, L., 1987: An improved wind input source term for third generation wave modelling. KNMI Scientific. Rept. WR-87-8.